ISSN 1990-7931, Russian Journal of Physical Chemistry B, 2019, Vol. 13, No. 1, pp. 75–85. © Pleiades Publishing, Ltd., 2019.
Russian Text © V.Ya. Basevich, A.A. Belyaev, S.M. Frolov, F.S. Frolov, 2019, published in Khimicheskaya Fizika, 2019, Vol. 38, No. 1, pp. 27–37.

COMBUSTION, EXPLOSION, AND SHOCK WAVES

Direct Numerical Simulation of Turbulent Combustion of Hydrogen–Air Mixtures of Various Compositions in a Two-Dimensional Approximation

V. Ya. Basevich[a], A. A. Belyaev[a], S. M. Frolov[a, b, c, *], and F. S. Frolov[a, c]

[a] *Semenov Institute of Chemical Physics, Russian Academy of Sciences, Moscow, 119991 Russia*
[b] *MIFI National Research Nuclear University, Moscow, 115409 Russia*
[c] *Systems Research Institute, Federal Scientific Center, Russian Academy of Sciences, Moscow, 117218 Russia*
**e-mail: smfrol@chph.ras.ru*

Received March 14, 2018; revised March 14, 2018; accepted March 20, 2018

Abstract—A technique of two-dimensional direct numerical simulation of turbulent flame propagation in reacting gas mixtures under stationary homogeneous isotropic turbulence conditions is proposed. This technique is based on a detailed kinetic mechanism of combustion of a multicomponent mixture and uses no fitting parameters. It is applied to the calculation of turbulent combustion of a hydrogen–air mixture. A condition is proposed to compare the results of two-dimensional calculations (dependences of flame propagation velocity on turbulence intensity) with the data of actual three-dimensional experiments. The obtained agreement between the calculated and measured dependences confirmed the validity of the proposed condition. The effects of pressure on the flame propagation velocity were considered. The calculated concentrations of the active reaction centers—hydroxyl (OH) and H and O atoms—in turbulent flame are lower than those in laminar flame, which also agrees with experimental results.

Keywords: direct numerical simulation, turbulent combustion, detailed kinetic mechanism, hydrogen

DOI: 10.1134/S1990793119010044

INTRODUCTION

Direct numerical simulation of turbulent combustion is performed using a nonempirical approach that is based on detailed kinetic mechanisms and accounts for the pulsation velocity field. The pioneering works on the mathematical modeling of turbulent combustion were published long ago [1, 2], but universally accepted methods of mathematical description of physicochemical processes in turbulent flame have not yet been developed [3–9]. The existing approaches, as a rule, include multifarious closing hypotheses that are based on experimental observations. Because the applicability domain of a hypothesis is limited, such semiempirical approaches are not universal. The most promising universal approach to nonempirical theoretical description of turbulent combustion is considered to be direct numerical simulation (DNS), which takes into account all the main features of a three-dimensional turbulent reacting flow with a full range of turbulent pulsations of velocity, with the full range of the initial, intermediate, and final chemical components and their individual thermochemical properties and molecular transfer properties, under adequate boundary conditions [7–9]. Constitutive flow equations are numerically integrated in computational grids that ensure the spatial resolution of Kolmogorov-scale turbulent eddies using high-order approximation schemes.

Despite the considerable progress that has been made in the development of the DNS of turbulent combustion, many problems remain for this method. For example, a comparison of the most recently published solutions for turbulent flame propagation velocity that have been obtained by DNS (see, e.g., [10]) with the known experimental data shows that the accuracy of the former is still noticeably inferior to the accuracy reached in solving laminar combustion problems. In theoretical works, the causes of the discrepancy between the calculated and experimental data are often thought to be unaccounted-for phenomena induced by indefinite boundary conditions in actual experiments. Moreover, the DNS of actual turbulent flames is highly computer intensive, meaning that calculations must include simplifications that influence the accuracy of the solution.

In this work, an alternative approach to the DNS of turbulent combustion of a homogeneous gas mixture was used; this solution was previously published [11]. Instead of numerically solving all the equations that determine the turbulent flame propagation in a react-

ing gas, it was proposed [11] to solve only the equations of the transfer of scalar quantities—the concentrations of reagents and the energy—in an artificial (synthetic) turbulence field, characterized by a given (constant) root mean square intensity of velocity pulsations and by given (constant) integral spatial and temporal scales. It was also assumed that the propagation of the flame does not influence the characteristics of the synthetic turbulence field in the preflame zone.

Unlike the previous study [11], in this work, chemical processes are described, not by a single overall reaction, but by a detailed kinetic mechanism involving active centers. The first results of such a simulation of turbulent combustion were presented [12] for the single specific composition of a hydrogen–air mixture, under the simplest conditions of stationary homogeneous isotropic turbulence. The purpose of this work was to improve the technique proposed in [12] and use it to calculate turbulent flame propagation in homogeneous hydrogen–air mixtures of various compositions at various pressures and compare the results of calculation with known experimental data.

MATHEMATICAL FORMULATION OF THE PROBLEM

The system of equations determining turbulent flame propagation is based on the Navier–Stokes equations in a three-dimensional formulation, the energy-conservation equation, and the continuity equations for all the chemical components in a mixture of ideal gases [13]:

$$\frac{\partial \rho}{\partial t} + \nabla(\rho \mathbf{v}) = 0,$$

$$\rho \frac{\partial \mathbf{v}}{\partial t} + \rho \mathbf{v} \nabla \mathbf{v} = -\nabla p + \rho \sum_{i=1}^{N} Y_i \mathbf{f}_i,$$

$$\rho \frac{\partial e}{\partial t} + \rho \mathbf{v} \nabla e = -\nabla \mathbf{q} - \mathbf{P} : (\nabla \mathbf{v}) + \rho \sum_{i=1}^{N} Y_i \mathbf{f}_i \mathbf{V}_i,$$

$$\rho \frac{\partial Y_i}{\partial t} + \rho \mathbf{v} \nabla Y_i = \omega_i - \nabla(\rho Y_i \mathbf{V}_i), \quad i = 1,\ldots,N, \qquad (1)$$

$$p = \rho R^0 T \sum_{i=1}^{N} \frac{Y_i}{\mu_i},$$

$$e = \sum_{i=1}^{N} h_i Y_i - \frac{p}{\rho},$$

$$h_i = h_i^0 + \int_{T_0}^{T} c_{p,i} dT, \quad i = 1,\ldots,N,$$

where t is time; ρ is the density; $\mathbf{v}$ is the velocity vector; p is the static pressure; e is the internal energy; $\mathbf{q}$ is the molecular heat flux vector; $\mathbf{P}$ is the pressure force tensor; $\mathbf{f}_i$ is the vector of the gravitational force acting on unit weight of the ith substance; Y_i, $\mathbf{V}_i$, h_i, and ω_i are the mass fraction, diffusion velocity vector, specific enthalpy, and chemical transformation rate of the ith species, respectively; h_i^0 is the standard enthalpy of formation of the ith species; N is the number of species in the reacting gas; R^0 is the universal gas constant; μ_i is the molecular weight of the ith species; T is temperature; $c_{p,i}$ is the specific heat at constant pressure of the ith species; ∇ is the nabla operator; and the subscript 0 indicates the initial conditions of the fresh mixture.

It is assumed that system (1) is complemented with a detailed kinetic mechanism of fuel oxidation, thermochemical data (h_i^0, $c_{p,i}$) on each of the species, corresponding relations for $\mathbf{f}_i$, $\mathbf{q}$, $\mathbf{P}$, $\mathbf{V}_i$, and $\boldsymbol{\omega}_i$, and initial and boundary conditions. Solving the problem should give a stationary propagation velocity u_t (turbulent combustion rate) and the structure of the turbulent flame in the multicomponent reacting gas. To simplify the solution of the problem, let us make the following main assumptions:

(1) The geometry of the flow region is simplest: the turbulence is stationary, homogeneous, and isotropic.

(2) The pressure is constant ($p = p_0$), and the effect of gravity can be neglected. Owing to these assumptions, the problem is significantly simplified because there is no need to solve the momentum conservation equation.

(3) The heat flux $\mathbf{q}$ is determined only by molecular heat conduction (radiant heat transfer can be neglected).

(4) Thermal diffusion is low.

(5) The reacting mixture is highly diluted with an inert gas (nitrogen); therefore, all the diffusion fluxes of all the chemical components are determined by Fick's law with the binary diffusion coefficient.

Under assumptions (2)–(5), the system of differential equations (1) reduces to the form

$$\frac{\partial \rho}{\partial t} + \nabla(\rho \mathbf{v}) = 0,$$

$$\rho \frac{\partial e}{\partial t} + \rho \mathbf{v} \nabla e = -\nabla(\lambda \nabla T), \qquad (2)$$

$$\rho \frac{\partial Y_i}{\partial t} + \rho \mathbf{v} \nabla Y_i = \omega_i - \nabla(D_i \rho \nabla Y_i), \; i = 1,\ldots,N,$$

where λ is the molecular thermal conductivity of the gas, and D_i is the binary diffusion coefficient of the ith species in nitrogen. Note that, owing to the second of the above assumptions, the density ρ in Eqs. (2) is a function of only temperature and the composition of the mixture.

To further simplify the problem, let us assume that the solution of system (2) tends to a certain stationary solution, for which

$$\nabla(\rho \mathbf{v}) = 0. \qquad (3)$$

Because it is a stationary solution that is required, Eq. (3) can be used instead of the continuity equations of the mixture; i.e., instead of the first equation of system (2). In this case, the formulation of the problem can be simplified still further. The instantaneous local velocity vector $\mathbf{v} = (u, v, w)$ in Eq. (3), where u, v, and w are the components of the vector, can be represented as the sum of the average velocity vector $\mathbf{V} = (U, V, W)$ and the velocity pulsation vector $\mathbf{v}' = (u', v', w')$:

$$\mathbf{v} = \mathbf{V} + \mathbf{v}'.$$

Here and hereinafter, capital letters denote average values, and primes refer to pulsations. Then, Eq. (3) can be transformed into the form

$$\nabla(\rho\mathbf{v}) = \nabla(\rho\mathbf{V} + \rho\mathbf{v}') = \nabla(\rho\mathbf{V}) + \nabla(\rho\mathbf{v}') = 0. \quad (4)$$

Based on the first assumption of homogeneous isotropic turbulence, let us assume that

$$\nabla(\rho\mathbf{v}') = 0, \quad (5)$$

and, hence,

$$\nabla(\rho\mathbf{V}) = 0. \quad (6)$$

In the flow region of the simplest geometry (see the first assumption), there always exists an averaged direction of turbulent flame propagation, in which one spatial coordinate axis can be directed. Then, Eq. (6) can be integrated to obtain

$$\rho\mathbf{V} = \rho_0\mathbf{V}_0 = \mathbf{B}, \quad (7)$$

where $\mathbf{B}$ is the constant flux of matter. Using Eqs. (7), system (2) can be transformed to the form

$$\rho\frac{\partial e}{\partial t} + \mathbf{B}\nabla e = -\nabla(\lambda\nabla T) - \nabla(\rho\mathbf{v}'u),$$
$$\rho\frac{\partial Y_i}{\partial t} + \mathbf{B}\nabla Y_i = \omega_i - \nabla(D_i\rho\nabla Y_i) - \nabla(\rho\mathbf{v}'Y_i), \quad (8)$$
$$i = 1,\ldots,N.$$

The last terms of both equations of system (8) determine the transfer of matter and energy with turbulent velocity pulsations. If the vector $\mathbf{B}$ is known, then the time derivatives in both equations of system (8) can be taken to be zero to obtain the structure of stationary turbulent flame. However, as a rule, the value of the vector $\mathbf{B}$ is unknown beforehand. Therefore, to find its value, it is necessary to solve nonstationary system (8), which describes the combustion wave propagation until reaching a certain constant velocity. In this case, the convective terms in system (8) can be omitted, and the system of equations takes the form

$$\rho\frac{\partial e}{\partial t} = -\nabla(\lambda\nabla T) - \nabla(\rho\mathbf{v}'e),$$
$$\rho\frac{\partial Y_i}{\partial t} = \omega_i - \nabla(D_i\rho\nabla Y_i) - \nabla(\rho\mathbf{v}'Y_i), \quad (9)$$
$$i = 1,\ldots,N.$$

Finally, the last terms of the two equations (9) can also be simplified by using Eq. (5) and assuming that

$$\nabla_x(\rho u') = \nabla_y(\rho v') = \nabla_z(\rho w') = 0, \quad (10)$$

where $\nabla_x = \frac{\partial}{\partial x}$, $\nabla_y = \frac{\partial}{\partial y}$, and $\nabla_z = \frac{\partial}{\partial z}$. Integration of Eqs. (10) gives

$$\rho u' = \rho_0 u_0',$$
$$\rho v' = \rho_0 v_0', \quad (11)$$
$$\rho w' = \rho_0 w_0',$$

The substitution of relations (11) in system (9) ultimately gives

$$\rho\frac{\partial e}{\partial t} = -\nabla(\lambda\nabla T) - \rho_0 c_v \mathbf{v}_0'\nabla T,$$
$$\rho\frac{\partial Y_i}{\partial t} = \omega_i - \nabla(D_i\rho\nabla Y_i) - \rho_0\mathbf{v}_0'\nabla Y_i, \quad (12)$$
$$i = 1,\ldots,N.$$

Thus, as before [11, 12], instead of numerically solving system (1), it is proposed to solve system (12), which comprises only the equations of transfer of scalar quantities—the concentrations of all N reagents and the energy—in a given synthetic turbulence field characterized by the root mean square intensity $\mathbf{v}'$ of velocity pulsations and by given integral spatial and temporal scales. As a first step, we can restrict ourselves to solving a two-dimensional problem, although the area of the flame surface in the two-dimensional approximation is smaller than that in the three-dimensional approximation, and two-dimensional turbulence affects the turbulent flame propagation less strongly than three-dimensional turbulence. In the two-dimensional approximation, in coordinate system (x, y), Eqs. (12) with account of the caloric equation take the form

$$\rho c_p\frac{\partial T}{\partial t} = \sum_{i=1}^{N} h_i\omega_i + \left(\frac{\partial}{\partial x}\lambda\frac{\partial T}{\partial x} + \frac{\partial}{\partial y}\lambda\frac{\partial T}{\partial y}\right) - \rho_0 c_p\left(u_0'\frac{\partial T}{\partial x} + v_0'\frac{\partial T}{\partial y}\right),$$
$$\rho\frac{\partial Y_i}{\partial t} = \omega_i + \left(\frac{\partial}{\partial x}D_i\rho\frac{\partial Y_i}{\partial x} + \frac{\partial}{\partial y}D_i\rho\frac{\partial Y_i}{\partial y}\right) - \rho_0\left(u_0'\frac{\partial Y_i}{\partial x} + v_0'\frac{\partial Y_i}{\partial y}\right), \quad i = 1,\ldots,N, \quad (13)$$
$$p_0 = \rho R^0 T\sum_{i=1}^{N}\frac{Y_i}{\mu_i}.$$

System (13) consists of $N + 2$ equations with $N + 2$ variables (N substances with mass fractions Y_i, temperature T, and density ρ). The system is closed by the following relations for c_p, λ, and D_i:

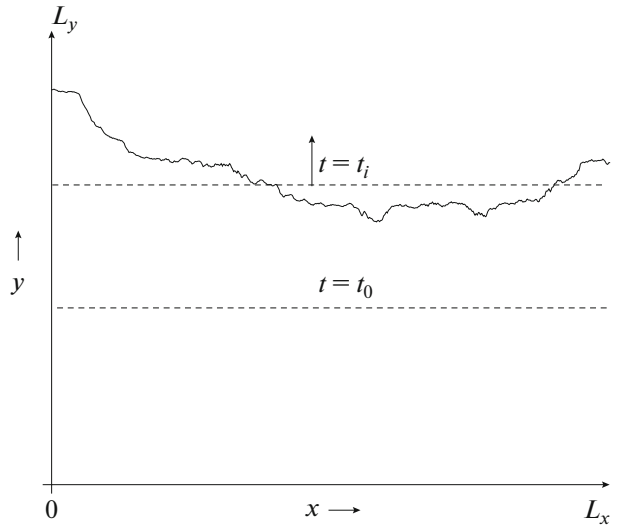

Fig. 1. Scheme of computational domain.

$$c_p = \sum_{i=1}^{N} c_{p,i} Y_i,$$

$$c_{p,i} = \frac{R^0}{\mu_i}\left(a_1 + a_2 T + a_3 T^2 + a_4 T^3 + a_5 T^4\right), \qquad (14)$$

$$\lambda = \lambda(T, Y_1, \ldots, Y_N, \mu_1, \ldots, \mu_N, c_{p,1}, \ldots, c_{p,N}),$$

$$D_i = D_i(T, p, \mu_i, \mu_{\text{in}}),$$

where a_1, a_2, a_3, a_4, and a_5 are coefficients of polynomials, and the subscript *in* denotes an inert diluent (nitrogen).

The chemical reaction rates are calculated as [13]

$$\omega_i = \mu_i \sum_{k=1}^{M} (\nu_{i,k}^- - \nu_{i,k}^+) A_k T^{\alpha_k}$$

$$\times \exp\left\{-(E_k / R^0 T)\right\} \prod_{j=1}^{N} \left(\frac{X_j p}{R^0 T}\right)^{\nu_{j,k}^+}, \quad i = 1, \ldots, N,$$

where $\nu_{i,k}^+$ and $\nu_{i,k}^-$ are the stoichiometric coefficients of the ith species—the initial substances and products of the kth reaction, respectively; A_k is the pre-exponential factor of the kth reaction; α_k is the exponent, which determines the temperature dependence of the pre-exponential factor of the kth reaction; E_k is the activation energy of the kth reaction; M is the total number of chemical reactions; and X_j is the mole fraction of the jth species.

Equations (13) contain parameters of the stationary homogeneous isotropic turbulence of the reacting gas (two components of the vector $\mathbf{v}_0' = (u_0', v_0')$). The components of the pulsation velocity vector can be obtained by random generation by the Monte Carlo method under the assumption that the instantaneous local components of the pulsation velocity vector have the normal Gaussian distribution φ and that the vortex structure of turbulence is described by the spatial (R' and R'') and temporal (R) exponentially decaying correlation functions:

$$\varphi(u') = \frac{1}{\sqrt{2\pi}\sigma} \exp\left[-\frac{(u' - \overline{u})^2}{2\sigma^2}\right], \qquad (15)$$

$$R' = \exp\left(-r_k / L'\right), \quad R'' = \exp\left(-r_k / L''\right), \quad R = \exp(-t/\tau), \qquad (16)$$

where u' is the instantaneous component of the pulsation velocity vector; $\overline{u}$ is the length of the vector of the average pulsation velocity; σ is the root–mean–square deviation of velocity pulsations; r_k is the distance in the physical space; L' and L'' are the turbulence length scales in the directions y and x, respectively; and τ is the Lagrangian time scale. Despite the assumption of the isotropy of the turbulence field (the first assumption, see above), here, for generality, two spatial scales, L' and L'', are introduced. Under the assumption of the stationarity and homogeneity of the turbulence field, the scales τ, L', and L'', are taken constant. The boundary and initial conditions of system (13) are considered below for a specific computational domain.

COMPUTATIONAL PROCEDURE

Figure 1 presents a scheme of the simplest computational domain in a chosen coordinate system (x, y). This computational domain is a rectangle, where the left and right boundaries are impermeable walls at which the flow slips, and the lower and upper boundaries are far away enough from the flame to ensure the constancy of the pressure in the system throughout the computation time. The initial position of the plane flame front at time $t = t_0 = 0$ is shown by the lower horizontal dashed line. The flame propagates bottom-up: above the dashed line is a fresh combustible mixture, and below it are the products of combustion. Here and hereinafter, at $t > 0$, the position of the combustion front is defined as the locus of points at which the temperature is equal to the arithmetic mean of the initial temperature T_0 of the fresh mixture and the thermodynamically equilibrium temperature T_1 of the combustion products $T_m = (T_0 + T_1)/2$.

The instantaneous position of the flame front at time $t = t_i > 0$ is shown by the continuous line, and its averaged position is represented by the upper horizontal dashed line, which is drawn so that the areas of the regions cut by the continuous curve above and below the dashed line are equal.

The problem of the turbulent flame propagation was solved by the numerical integration of system (13) with additional relations by the alternating direction method of multipliers [14]. The equations in each of the directions (x, y) were solved using an implicit difference scheme with uniform spatial steps and linearization of nonlinear source terms in the upper layer.

This scheme was of the first order of accuracy in time and space. The computational domain had the size 0.5×4 cm^2. Each of the computational cells had the shape of a square 0.005×0.005 cm^2 in size. The total number of computational cells was 80 000. The time integration step was varied, depending on the number of iterations, but did not exceed 10^{-6} s.

An important operation was to model the synthetic turbulence field $\mathbf{v}'_0 = (u'_0, v'_0)$ in system (13). The pulsation velocity fields $u' = u'_x(x, y, t)$ and $v' = u'_y(x, y, t)$ were modeled by their random generation at given turbulence characteristics $\overline{u}$, L', L'', and τ according to the procedure described in the Appendix. Note that the procedure used for constructing the synthetic turbulence field did not require one to define either the turbulence spectrum or the Kolmogorov scale. The instantaneous length of the pulsation velocity vector u was found from the values of u'_x and u'_y:

$$u = \left[(u'_x)^2 + (u'_y)^2\right]^{1/2}.$$

The following initial and boundary conditions were used:

$$\begin{gathered} t = t_0 = 0, \quad y > y(t = t_0)\colon Y_j = Y_{j0}, T = T_0, \\ j = 1,\ldots,N, \\ y < y(t = t_0)\colon Y_j = Y_{j1}, \quad T = T_1, j,\ldots,N; \end{gathered} \tag{17}$$

$$\begin{gathered} x = 0\colon \frac{\partial T}{\partial x} = 0, \quad \frac{\partial Y_j}{\partial x} = 0, \quad j = 1,\ldots,N, \\ x = L_x\colon \frac{\partial T}{\partial x} = 0, \quad \frac{\partial Y_j}{\partial x} = 0, \quad j = 1,\ldots,N, \\ y = 0\colon \frac{\partial T}{\partial y} = 0, \quad \frac{\partial Y_j}{\partial y} = 0, \quad j = 1,\ldots,N, \\ y = L_y\colon \frac{\partial T}{\partial y} = 0, \quad \frac{\partial Y_j}{\partial y} = 0, \quad j = 1,\ldots,N. \end{gathered} \tag{18}$$

COMPUTATION RESULTS

As previously [12], in this work, the turbulent combustion of a homogeneous hydrogen–air mixture was considered. The chemical transformation kinetics was described using a set of hydrogen oxidation reactions with detailed kinetic mechanisms of oxidation and the combustion of normal hydrocarbons [15]. The values of the coefficients of the polynomials for all the substances were taken from the database [16]. The transfer coefficients $\boldsymbol{\lambda}$ and D_i were calculated according to a published procedure [17].

Prior to solving the problem of turbulent flame propagation, system (13) was numerically integrated under initial and boundary conditions (17) and (18) without synthetic turbulence, i.e., at zero pulsation velocities $\mathbf{v}'_0 = (u'_0, v'_0) = 0$, to test the applicability of the technique to describing the plane laminar flame propagation at velocity u_n. The computations were performed for $T_0 = 293$ K and $p = 1$ ata. The hydrogen volume content of the mixture was varied from 9.09 to 23.09%. In Fig. 2, the results of these computations are represented by symbols *1*. Figure 2 compares the obtained results with experimental data [3, 18–23] and with the results of calculation using a published program [24] over a wider range of hydrogen volume contents from 6 to 75%. Experimental data are available on both laminar and turbulent flames in mixtures with hydrogen volume contents from 9.09 to 23.09% [18]. Below, these data [18] were used to compare the dependences of the calculated and measured velocities of turbulent combustion of mixtures of various compositions on turbulence intensity. For hydrogen–air mixtures containing less than 9.0% H_2, a stationary solution for plane laminar flame failed to be obtained.

Figure 3 gives examples of the instantaneous shape of the turbulent flame front at various times after the start of computations. The maximal physical time for computing the turbulent flame reached 10^{-3} s; i.e., it was shorter than the characteristic temporal scale τ. The curves in Fig. 3 are individual realizations of the position of the turbulent flame front. In the flame front, both small and large spatial inhomogeneities are observed. As shown below, they are characterized by linear sizes that are both smaller and larger than the flame front thickness. Small-scale turbulence changes (increases) the rate of transfer processes (exchange of mass and energy) within the flame front, and large-scale turbulence changes the shape of the flame and increases its surface area.

Despite a relatively short physical time of computation ($t < \tau$), the obtained value of the propagation velocity of the averaged turbulent flame is almost time constant (Fig. 4). From the flame front positions averaged over several realizations (usually 5–7 realizations), the visible velocity U of the propagation of the flame front at a given pulsation velocity can be found. Taking the thermal expansion of the reaction products into account, it is possible to determine the propagation velocity of the turbulent flame

$$u_t = U \frac{T_0}{T_1} \frac{m_0}{m_1},$$

where m_0 and m_1 are the numbers of moles in the fresh mixture and the reaction products, respectively.

Figure 5 compares the calculated and measured dependences of the propagation velocity of turbulent flame u_t in mixtures of various compositions on the root–mean–square pulsation velocity $\overline{u}$. Importantly, in Fig. 5, as in the experimental work [18], the abscissa is the root–mean–square pulsation velocity $\overline{u} = \sqrt{3}u'$, where u' is the projection of $\overline{u}$ on the y axis. According to Eqs. (4), for correct comparison of the results of two-dimensional calculations with the data of real "three-dimensional" experiments, the abscissa should

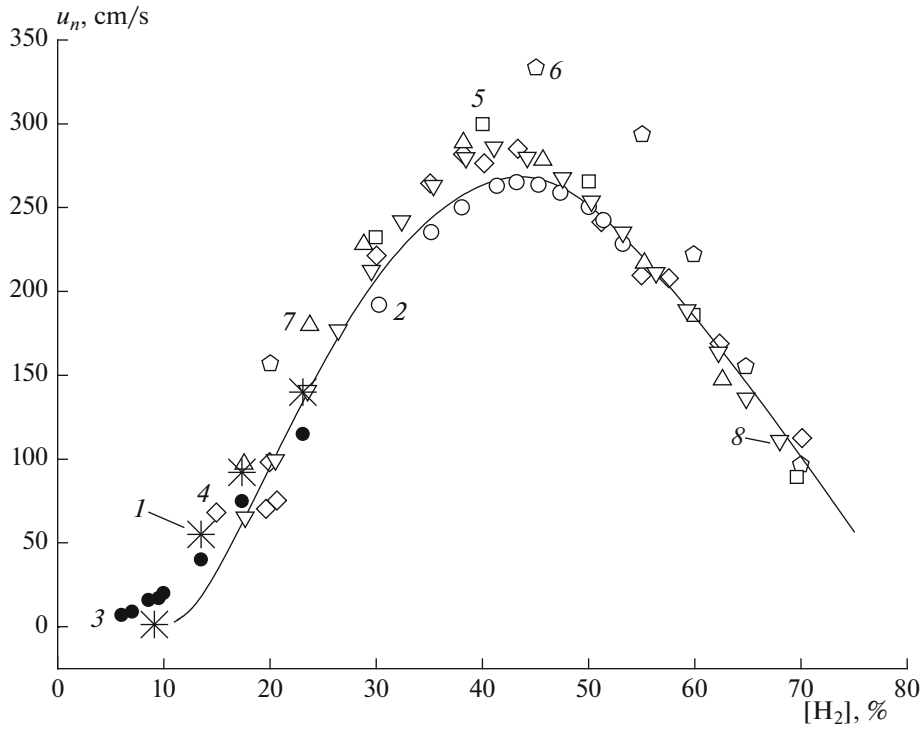

Fig. 2. Comparison of the calculated and measured values of the laminar flame propagation velocity u_n on the composition of the hydrogen–air mixture. Initial temperature $T_0 = 293$ K, atmospheric pressure. (*1*) Results of calculations in this work and experimental points (*2*) [3], (*3*) [18], (*4*) [19], (*5*) [20], (*6*) [21], (*7*) [22], and (*8*) [23]; the curve represents the results of the calculation [24].

be $\overline{u} = \sqrt{2}u$; i.e., for the calculated values of the pulsation velocity, the linear scale should be reduced in the ratio $\sqrt{2} : \sqrt{3} \approx 0.815$. It is this condition that enables one to compare the results of two-dimensional calcu-

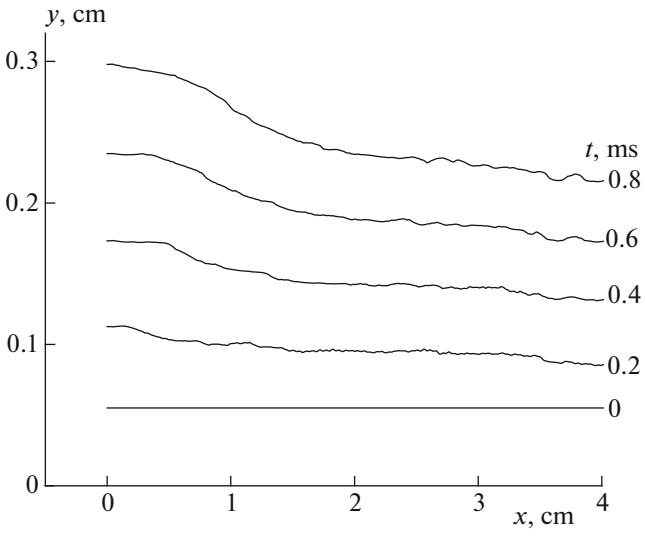

Fig. 3. Calculated positions of the turbulent flame front in various times (t = 0–0.8 ms). Hydrogen–air mixture; fuel–air equivalence ratio $\Phi = 0.5$ (H_2 volume content 17.36%); initial temperature $T_0 = 293$ K; atmospheric pressure; and turbulence characteristics: $\overline{u} = 130$ cm/s, $L' = 1$ cm, $L'' = 0.7$ cm, and $\tau = 0.010$ s.

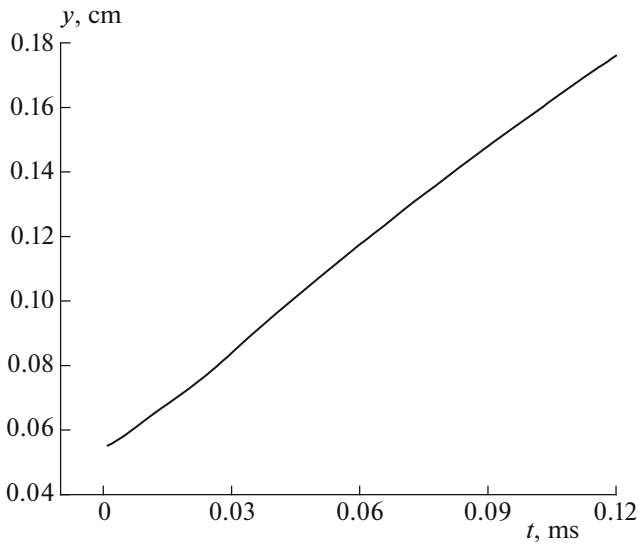

Fig. 4. Calculated dependence of the distance travelled by the averaged turbulent flame front on time. Hydrogen–air mixture; fuel–air equivalence ratio $\Phi = 0.5$; initial temperature $T_0 = 293$ K; atmospheric pressure; and turbulence characteristics: $\overline{u} = 660$ cm/s, $L' = 1$ cm, $L'' = 0.7$ cm, and $\tau = 0.010$ s.

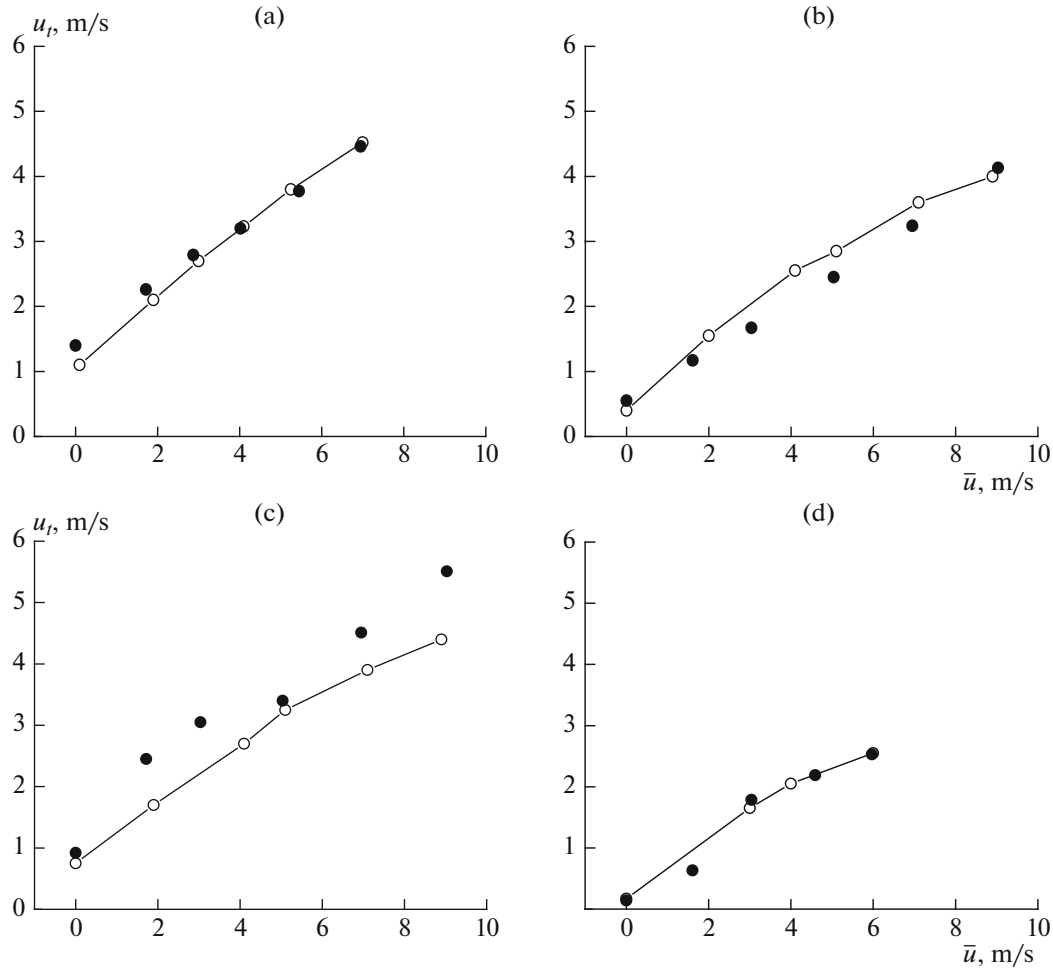

Fig. 5. Calculated (filled circles) and measured [18] (open circles with lines) dependences of the turbulent flame propagation velocity u_t on the root–mean–square pulsation velocity $\bar{u}$. Hydrogen–air mixtures containing (a) 23.09, (b) 13.51, (c) 17.36, and (d) 9.09% H_2; initial temperature $T_0 = 293$ K; atmospheric pressure; and turbulence characteristics: $L' = 1$ cm, $L'' = 0.7$ cm, and $\tau = 0.010$ s.

lations with the data of "three-dimensional" experiments. This comparison of the calculated and measured data shows that they agree satisfactorily.

Figure 6 compares the calculated temperature profiles in the laminar and turbulent flames (instantaneous realization). Using these profiles, the flame thickness can be estimated and compared with the spatial scales of velocity pulsations. The temperature profile in the turbulent flame is shallower than that in the laminar flame, and the turbulent flame is wider than the laminar flame because of the influence of small-scale exchange processes.

Figure 7 gives examples of the calculated profiles of temperature and the concentrations of the intermediate and final reaction products in the turbulent flame (instantaneous realization). Although the structures of the reaction zones in the turbulent and laminar flames are similar, there are nonetheless some qualitative differences. For example, the concentrations of the most active intermediate products—hydroxyl (OH) and H and O atoms—in the turbulent flame are lower than those in the laminar flame. This is clearly seen in Fig. 8, which presents examples of the calculated dependences of the maximal (throughout the reaction zone) hydroxyl concentrations on the root–mean–square pulsation velocity $\bar{u}$. The decrease in the concentration of active centers is a consequence of the increase in the turbulence intensity, i.e., the acceleration of exchange processes. The same conclusion was drawn in the earlier experiments based on the [25], based on indirect data.

It is well known that, with increasing pressure, the propagation velocity of the laminar flame decreases, and the propagation velocity of the turbulent flame either remains constant or somewhat increases [5]. The latter can also be seen in the results of our calculations of the propagation of turbulent flames at various pressures. Figure 9 compares the calculated dependences of the propagation velocities of the laminar and turbulent flames.

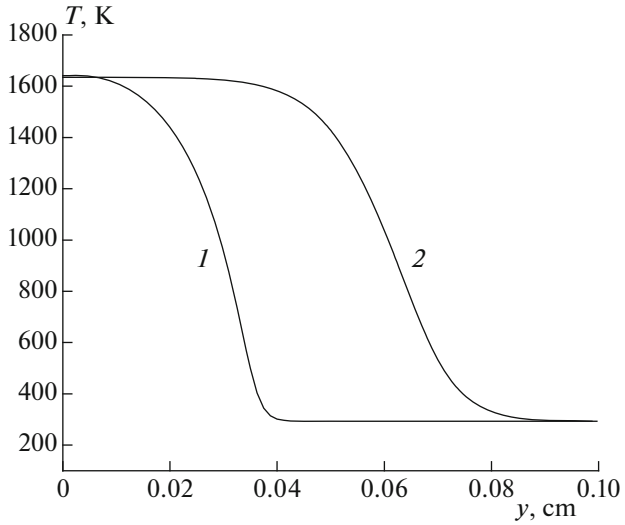

Fig. 6. Calculated temperature profiles in the (*1*) laminar and (*2*) turbulent flames. Hydrogen–air mixture, fuel–air equivalence ratio $\Phi = 0.5$, initial temperature $T_0 = 293$ K, and atmospheric pressure. The turbulence characteristics for the turbulent flame are $\bar{u} = 1100$ cm/s, $L' = 1$ cm, $L'' = 0.7$ cm, and $\tau = 0.010$ s.

In conclusion, we emphasize one result that is important for understanding the structure of the combustion zone in a turbulent flame: the surface of the flame in all the performed computations was connected simply. Even at the maximal turbulence intensities, the computations did not show the presence of pockets of the fresh combustible mixture, surrounded by the combustion products that have been described in the literature [10]. This is probably due to differences in methods of describing the synthetic turbulence field or to insufficiently long simulation of the turbulent flame propagation. This issue will be studied elsewhere.

CONCLUSIONS

The technique of the two-dimensional DNS of turbulent flame propagation in reacting gas mixtures under stationary homogeneous isotropic synthetic turbulence conditions was proposed. The technique is based on the detailed kinetic mechanism of combustion of a multicomponent mixture and uses no fitting parameters. The technique was applied to the calculation of the turbulent combustion of hydrogen–air mixtures of various compositions at various initial pressures. The condition was proposed to compare the results of the two-dimensional calculations with the data of actual experiments.

The comparison of the results of calculation with experimental data demonstrated a satisfactory qualitative agreement between them: both calculated and experimental turbulent combustion velocities increase

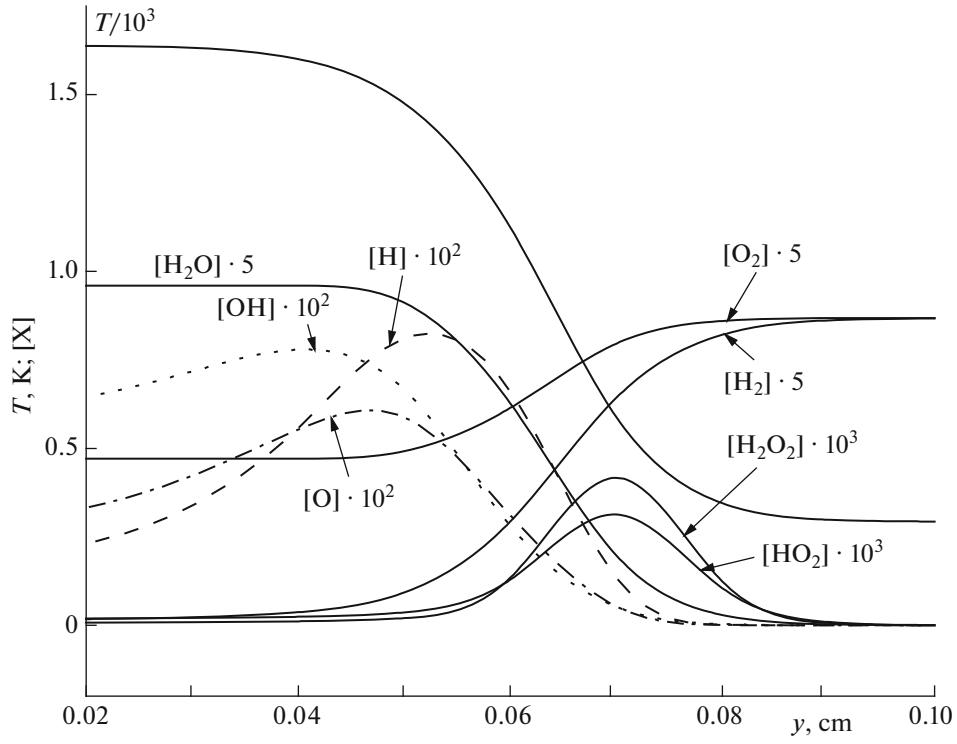

Fig. 7. Calculated profiles of temperature and the concentrations (volume fractions) [X] of some species in the turbulent flame. Hydrogen–air mixture; fuel–air equivalence ratio $\Phi = 0.5$; initial temperature $T_0 = 293$ K; atmospheric pressure; and turbulence characteristics: $\bar{u} = 1100$ cm/s, $L' = 1$ cm, $L'' = 0.7$ cm, and $\tau = 0.010$ s.

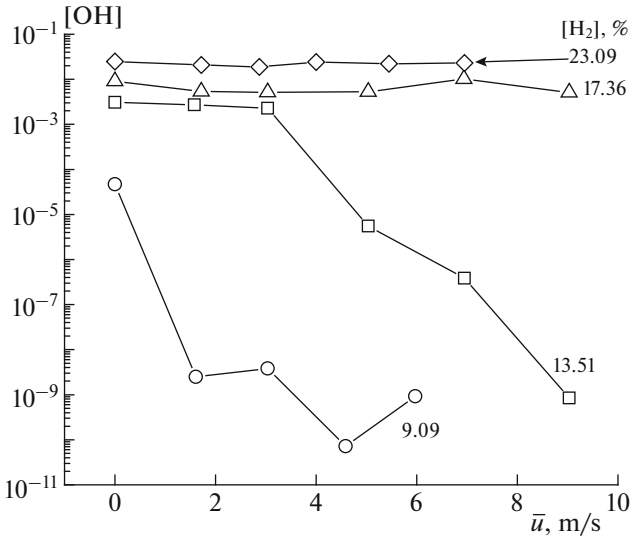

Fig. 8. Calculated dependences of the hydroxyl concentration (volume fraction) [OH] on the root–mean–square pulsation velocity $\bar{u}$. Hydrogen–air mixtures of various compositions; initial temperature $T_0 = 293$ K; atmospheric pressure; and turbulence characteristics: $L' = 1$ cm, $L'' = 0.7$ cm, and $\tau = 0.010$ s.

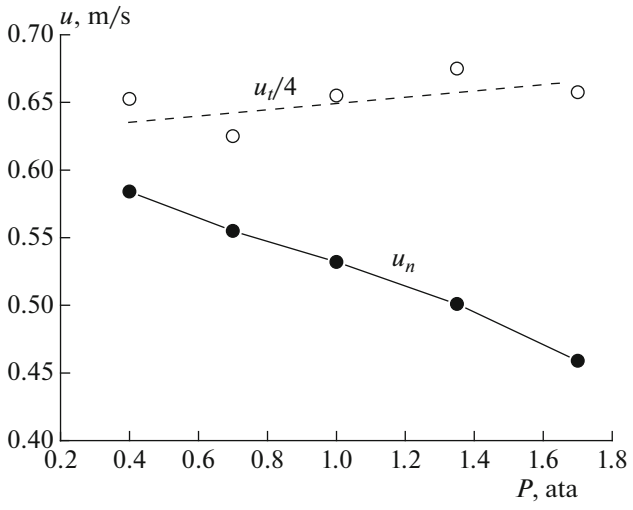

Fig. 9. Calculated dependences of the laminar flame propagation velocity u_n and the turbulent flame propagation velocity u_t on pressure. Hydrogen–air mixture, fuel–air equivalence ratio $\Phi = 0.5$, and initial temperature $T_0 = 293$ K. Turbulence characteristics for u_t: $\bar{u} = 510$ cm/s, $L' = 1$ cm, $L'' = 0.7$ cm, and $\tau = 0.010$ s.

with increases in the intensity of turbulence. The pressure dependence of the velocity of the turbulent flame propagation is also represented correctly. The calculations showed that the concentrations of active reaction centers—hydroxyl (OH) and H and O atoms—in the turbulent flame are lower than those in the laminar flame, which also agrees with the experimental results. The obtained qualitative agreement confirmed the applicability of the proposed condition to comparing the results of two-dimensional calculations with data from real experiments. Our further investigations will expand the proposed technique to the three-dimensional case and take into account the vortex structure of turbulence.

APPENDIX

Modeling of the Synthetic Turbulence Field

Geometric fields: x is the width (pulsation scale L''); y is the flame propagation direction (pulsation scale L'); Δx_k and Δt are the space and time integration steps, respectively; $k = 1, 2$ ($x_1 = x$, $x_2 = y$).

(1) Calculation of $u_x(x = 0, ..., N; y = 0; t = 0)$:

—at the point $(x = 0, y = 0, t = 0)$, according to a given value of $\bar{u}$, a random number generator provides $u_x(0, 0, 0)$; here and hereinafter, prior to any call of the random number generator, the average value (**AV**) should be tested: if $|\mathbf{AV}| > u$ (specified under the initial conditions), then one should take $|\mathbf{AV}| = u$;

—at the point $(x = \Delta x_1, 0, 0)$, the R'' value, the mean of the pulsation velocity $u_x(0, 0, 0)R''$, and the variance $\bar{u}^2(1 - R''^2)$ are calculated, and the pulsation velocity $u_x(\Delta x_1, 0, 0)$ is randomly tested;

—similarly, at intervals Δx_i to the end x of the computational segment, $u_x(1, 0, 0)$, $u_x(2, 0, 0)$, ..., $u_x(N, 0, 0)$ are determined.

(2) Calculation of $u_y(x = 0, ..., N; y = 0; t = 0)$:

—at the point $(x = 0, y = 0, t = 0)$, according to a given value of $\bar{u}$, the random number generator provides $u_y(0, 0, 0)$;

—at the point $(x = \Delta x_1, 0, 0)$, the R'' value, the mean of the pulsation velocity $u_y(0, 0, 0)R''$, and the variance $\bar{u}^2(1 - R''^2)$ are calculated, and the pulsation velocity $u_y(\Delta x_1, 0, 0)$ is randomly tested;

– similarly, at intervals Δx_i to the end x of the computational segment, $u_y(1, 0, 0)$, $u_y(2, 0, 0)$, ..., $u_y(N, 0, 0)$ are determined.

(3) Calculation of $u_y(x = 0,..., N; y = 1; t = 0)$:

—using the u_x values obtained at step (1), at points 1, 2, ..., N, the derivatives $\partial u_x/\partial x$ are calculated throughout the axis $x(0 - N, 0, 0)$;

—by the continuity equation, the derivatives $\partial u_y/\partial y$ are determined throughout the axis x $(0 - N, 0, 0)$;

—at the point $(x = 0, 1, 0)$,

$$\langle u_y(0,1,0)\rangle = u_y(0,0,0) + \{[\partial u_y/\partial y](0,0,0)\}\Delta y_1$$

is calculated;

—at the point ($x = 0$, $y = 1$, $t = 0$), the R' value, the mean of the pulsation velocity $[\langle u_y\ (0,\ 1,\ 0)\rangle]R'$, and the variance $\overline{u}^2(1 - R'^2)$ are calculated, and the probable value of the pulsation velocity $u_y(0,\ 1,\ 0)$ is randomly tested;

—similarly, at intervals Δx_i to the end x of the computational segment, $u_y(1,\ 1,\ 0)$, $u_y(2,\ 1,\ 0)$, ..., $u_y(N,\ 1,\ 0)$ are determined;

—for all $u_y(N,\ 1,\ 0)$, the root mean square $\langle u_y\ (0,..., N,\ 1,\ 0)\rangle$ is calculated, and the correction coefficient

$$a_u = \langle u_y(N,1,0)\rangle / \overline{u}$$

is determined, and the corrected values of $u_y(0,\ ...,\ N;\ 1;\ 0) = u_y(0,\ ...,\ N;\ 1;\ 0)/a_u$ are found.

(4) Calculation of $u_x(x = 0,\ ...,\ N;\ y = 1;\ t = 0)$:

—using the u_y values obtained at steps (1) and (3), at the points 1, 2, ..., N, the derivatives $\partial u_y/\partial y$ are determined throughout the axis $x(0,\ ...,\ N;\ 0;\ 0)$;

—by the continuity equation, the derivatives $\partial u_x/\partial x$ are determined throughout the axis $x(0,\ ...,\ N;\ 1;\ 0)$;

—at the point ($x = 0$, $y = 1$, $t = 0$) , according to a given value of $\overline{u}\,\overline{u}$, the random number generator provides $u_x\ (0,\ 1,\ 0)$;

—at the point ($x = 1,\ 1,\ 0$),

$$\langle u_x(1,1,0)\rangle = u_x(0,1,0) + \{[\partial u_x/\partial x]\}(1,1,0)\,\Delta x_1$$

is calculated;

—at the point ($x = 1$, $y = 1$, $t = 0$), the R'' value, the mean of the pulsation velocity $[\langle u_x(1,\ 1,\ 0)\rangle]R''$, and the variance $\overline{u}^2(1 - R''^2)$ are calculated, and the probable value of the pulsation velocity $u_x\ (1,\ 1,\ 0)$ is randomly tested;

—similarly, at intervals Δx_i to the end x of the computational segment, $u_x(1,\ 1,\ 0)$, $u_x(2,\ 1,\ 0)$, ..., $u_x(N,\ 1,\ 0)$ are determined;

—at all $u_x(N,\ 1,\ 0)$, the root mean square $\langle u_x\ (0,..., N,\ 1,\ 0)\rangle$ is calculated, and the correction coefficient

$$a_{ux} = \langle u_x(N,1,\ 0)\rangle / \overline{u}$$

is determined, and the corrected values of $u_x\ (0,..., N,\ 1,\ 0) = u_x\ (0,..., N,\ 1,\ 0)/a_{ux}$ are found.

(5) Calculation of $u_x(x = 0,\ ...,\ N;\ y = 1,\ ...,\ N;\ t = 0)$:

—as at steps (1)–(4).

(6) Calculation of $u_x(x = 0,\ ...,\ N, y = 1,\ ...,\ N, t = 0,\ ...,\ t_{end})$ and $u_y(x = 0,\ ...,\ N,\ y = 1,\ ...,\ N,\ t = 0,\ ...,\ t_{end})$:

—as the values of u_x and u_y change in the transition from the axis $x(0,\ ...,\ N;\ 0;\ 0)$ to the axis $x(0,\ ...,\ N;\ 1;\ 0)$, so they change in the transition from the axis $x(0,\ ...,\ N,\ 0,\ 0)$ to the axis $x\ (0,\ ...,\ N,\ 0,\ 1)$ but using the correlation coefficient $\boldsymbol{\tau}$. This technique is performed throughout the calculation: from $t = 0$ to t_{end}.

Validation of the algorithm. The obtained pulsation velocity fields should be checked for compliance to given turbulence characteristics $\overline{u}$, to a normal Gaussian distribution, and scales L', L'', and τ.

Note. From the assumption that turbulent pulsations meet conditions (10), the relationship between "cold" (subscript *0*) and "hot" ($T > T_0$) pulsations of velocity follows:

$$\rho u_k = \rho_0 u_{k,0},$$

where $u_{k,0}$ are the projections of the instantaneous pulsation velocity on the axis x_k at the initial density. This equation determines the change in the turbulence intensity in the course of the combustion, and random testing of velocity pulsations is required only at the initial temperature.

According to the algorithm of modeling the synthetic turbulence field, the root mean square pulsation velocity $\overline{u}$ is time-constant, and throughout the computational space, the turbulence characteristics L', L'', and $\boldsymbol{\tau}$ are constant.

ACKNOWLEDGMENTS

This work was supported in part by the Russian Foundation for Basic Research (project no. 16-29-01065 ofi-m) and the Semenov Institute of Chemical Physics, Russian Academy of Sciences, Moscow, Russia, in the performance of state assignments of the Federal Agency for Scientific Organizations (subject nos. 0082-2016-0011, AAA-A17-117040610346-5 and 0082-2014-0004, AAA-A17-117040610283-3).

REFERENCES

1. G. Damkoler, Z. Elektrochem. **46**, 601 (1940).
2. K. I. Shchelkin, Zh. Tekh. Fiz. **13**, 520 (1943).
3. B. Lewis and G. Elbe, *Combustion, Flames and Explosions of Gases* (Academic, Orlando, 1987).
4. A. S. Sokolik, *Self-Ignition, Flame and Detonation in Gases* (Akad. Nauk SSSR, Moscow, 1960) [in Russian].
5. E. S. Shchetinkov, *Gas Combustion Physics* (Nauka, Moscow, 1965) [in Russian].
6. J. A. Bernard and J. N. Bradley, *Flame and Combustion* (Chapman Hall, London, New York, 1985).
7. T. Echekki and J. H. Chen, Combust. Flame **134**, 169 (2003).
8. J. B. Bell, M. S. Day, and J. F. Grcar, Proc. Combust. Inst. **29**, 1987 (2002).
9. J. B. Bell, R. K. Cheng, M. S. Day, and I. G. Shepherd, Proc. Combust. Inst. **31**, 1309 (2006).
10. A. J. Aspden, M. S. Day, and J. B. Bell, Combust. Flame **166**, 266 (2016).
11. V. Ya. Basevich, V. P. Volodin, S. M. Kogarko, and N. I. Peregudov, Khim. Fiz. **1**, 1130 (1982).
12. V. Ya. Basevich, A. A. Belyaev, S. M. Frolov, and B. Basara, Gorenie Vzryv **10**, 4 (2017).
13. F. A. Williams, *Combustion Theory* (Addison-Wesley, Reading, Mass., 1965; Nauka, Moscow, 1971).
14. S. K. Godunov and V. S. Ryaben'kii, *Difference Schemes* (Nauka, Moscow, 1977) [in Russian].

15. V. Ya. Basevich, A. A. Belyaev, V. S. Posvyanskii, and S. M. Frolov, Russ. J. Phys. Chem. B **7**, 161 (2013).

16. A. Burcat, Thermodynamic Data at the Web Site of the Laboratory for Chemical Kinetics. Ideal Gas Thermodynamic Data in Polynomial Form for Combustion and Air Pollution Use. http://garfield.chem.elte.hu/Burcat/burcat.html.

17. R. C. Reid, J. M. Prausnitz, and T. K. Sherwood, *The Properties of Gases and Liquids* (McGraw-Hill, New York, 1977).

18. V. P. Karpov and E. S. Severin, Fiz. Goreniya Vzryva **16**, 45 (1980).

19. L. S. Kozachenko, Doctoral (Phys. Math.) Dissertation (Inst. Chem. Phys. Acad, Sci. USSR, Moscow, 1954).

20. J. Manton and B. B. Milliken, in *Proceedings of the Gas Dynamics Symposium on Aerothermochemistry, Northwestern Univ., 1956,* p. 151.

21. G. E. Andrews and D. Bradley, Combust. Flame **20**, 77 (1973).

22. T. Iijima and T. Takeno, Combust. Flame **65**, 35 (1986).

23. D. R. Dowdy, D. B. Smith, S. C. Taylor, and A. Williams, Proc. Combust. Inst. **23**, 325 (1990).

24. A. A. Belyaev and V. S. Posvyanskii, Algoritmy Program. Inform. Byull. Gos. Fonda Algoritmov Programm SSSR, No. 3, 35 (1985).

25. V. Ya. Basevich and S. M. Kogarko, Fiz. Goreniya Vzryva **21** (5), 12 (1985).

Translated by V. Glyanchenko